Bubble collapse near porous plates: Supplementary Material

Elijah D. Andrews†[1], David Fernández Rivas[2] and Ivo R. Peters[1]

January 20, 2023

[1]Faculty of Engineering and Physical Sciences, University of Southampton, Southampton SO17 1BJ, UK
[2]Mesoscale Chemical Systems Group, MESA+ Institute, TechMed Centre and Faculty of Science and Technology, University of Twente, P.O. Box 217, 7500 AE Enschede, The Netherlands

† Email address for correspondence: e.d.andrews@soton.ac.uk

1 Bubble statistics

Figure 1 shows histograms of some key bubble statistics. Data is compared between slots, using a microscope objective (MO), and porous plates, using an off-axis parabolic mirror (OAPM). The slots data are from our previous work (Andrews *et al.*, 2020). Each combination of geometry and position was repeated at least three times. Radius offset from mean and displacement offset from mean were both calculated as the offsets of each bubble from the mean of bubbles with the same geometry and position combination.

Due to the wider focusing angle, the off-axis parabolic mirror could produce consistently larger bubbles than the microscope objective as seen in the histogram of radii. For the same reason, the sphericity of the bubbles (measured by the eccentricity) was much improved by the off-axis parabolic mirror. The repeatability of bubbles was also improved by the off-axis parabolic mirror, as seen by the much tighter distribution of radius and displacement at each position.

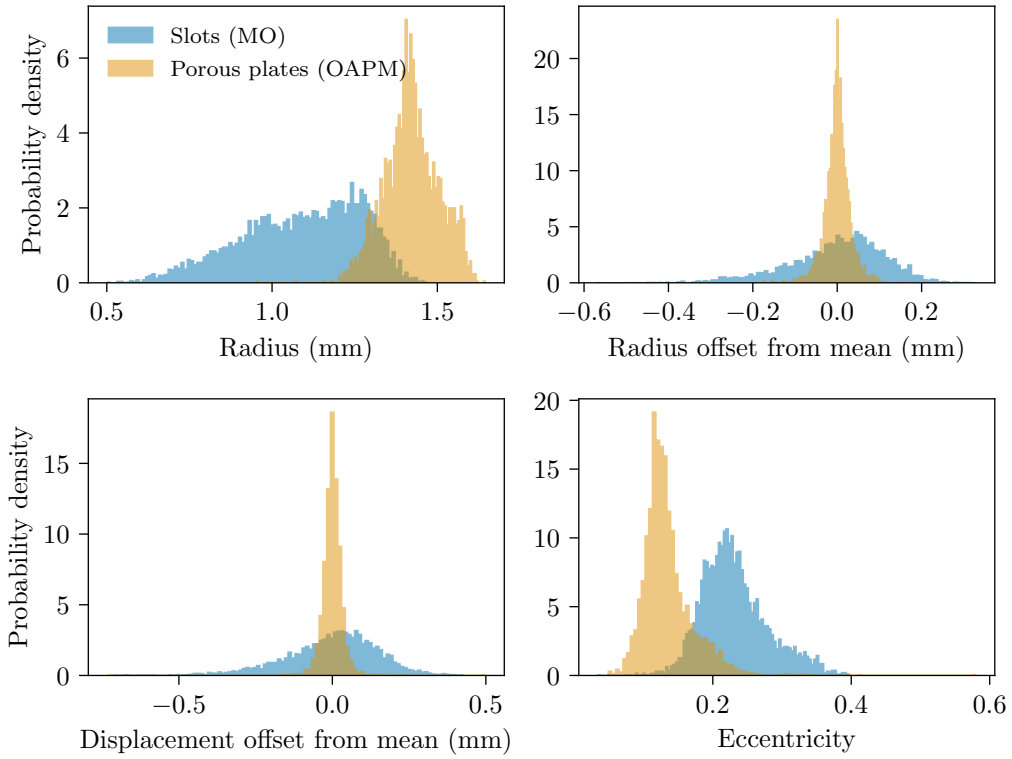

Figure 1: Histograms comparing bubble statistics between data from slot geometries using a microscope objective (MO) and porous plates data using an off-axis parabolic mirror (OAPM).

2 Numerical method area reduction description

The boundary element method represents a boundary as an infinite distribution of point sinks. This infinite distribution is discretised into boundary elements, shown in blue on figure 2. Each element is represented by a single point sink at its centroid, shown in purple on figure 2. Each element induces a velocity at a point in the fluid proportional to the element sink strength density σ_i and the element area A_i. Mathematically, no information is stored relating to the shape of the element beyond the

calculated area A_i.

In this work, we assume that the boundary has negligible thickness. Thus, we can use a single layer of elements to represent the boundary. For a non-porous boundary, these elements could be simple squares covering the whole boundary such as those shown in blue on figure 2. A porous boundary is similar, but has holes through the boundary. These holes could be represented by removing some panels, or redistributing panels to create holes. However, mathematically, this would simply redistribute the boundary element sinks at each centroid. Instead, the area of each element can be reduced so that each element no longer covers the full area of the boundary. These reduced-area elements are shown in green on figure 2. One could imagine that the white areas are 'holes', thereby creating a porous boundary.

In actuality, these 'holes' could be anywhere within the element so long as the total area is the same. One could imagine any shape of holes being created this way. Therefore, we say that this methodology assumes that the shape of holes doesn't matter.

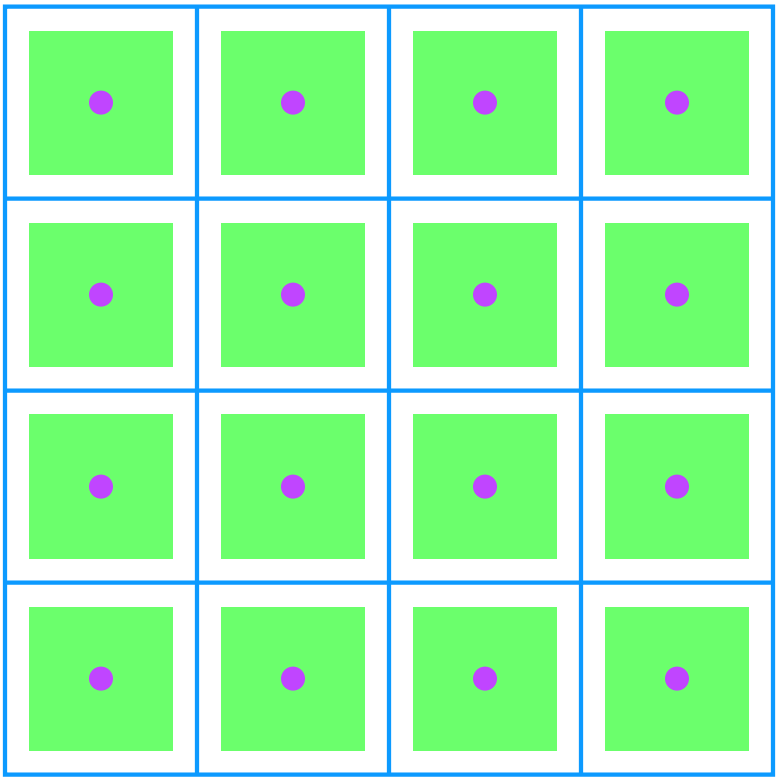

Figure 2: A diagram showing how porous boundary elements are represented. The blue squares show elements of area A_{is}, representing a non-porous boundary. The green squares are elements of a porous boundary with void fraction $\phi = 43.75$ %, each with area A_i. The purple dots show the centroid of each element.

3 All experimental data plots

This section contains displacement and rebound size plots for each plate individually. Data are plotted with the same axis bounds for ease of comparison.

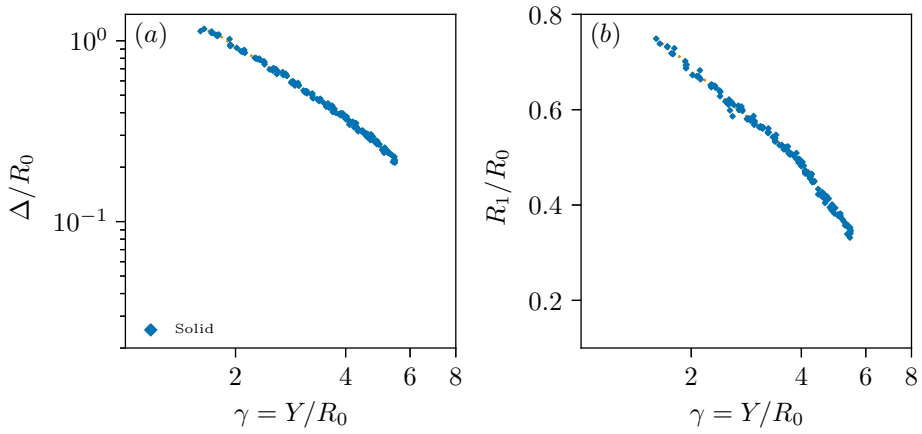

Figure 3: (a) Normalised displacement plotted against standoff distance. (b) Normalised rebound radius plotted against standoff distance. Data are plotted for a solid plate.

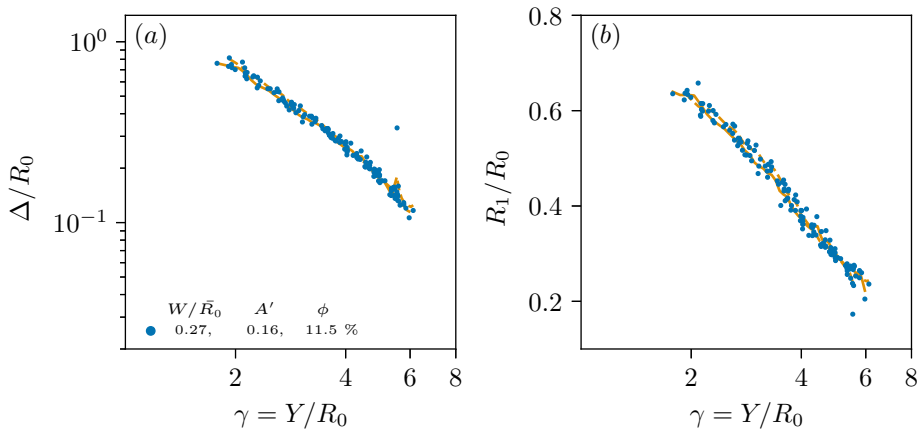

Figure 4: (a) Normalised displacement plotted against standoff distance. (b) Normalised rebound radius plotted against standoff distance. Data are plotted for a porous plate with circular holes. Data for bubbles positioned between-holes are traced by solid lines and data for bubbles positioned above holes are traced by dashed lines.

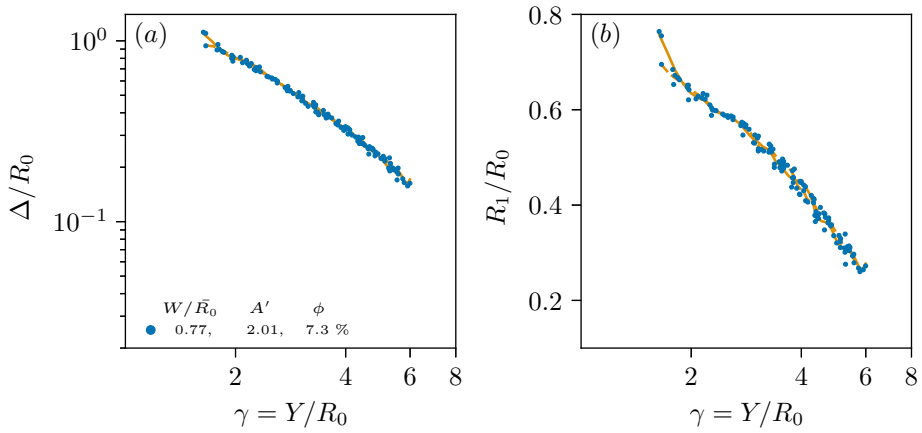

Figure 5: (a) Normalised displacement plotted against standoff distance. (b) Normalised rebound radius plotted against standoff distance. Data are plotted for a porous plate with circular holes. Data for bubbles positioned between-holes are traced by solid lines and data for bubbles positioned above holes are traced by dashed lines.

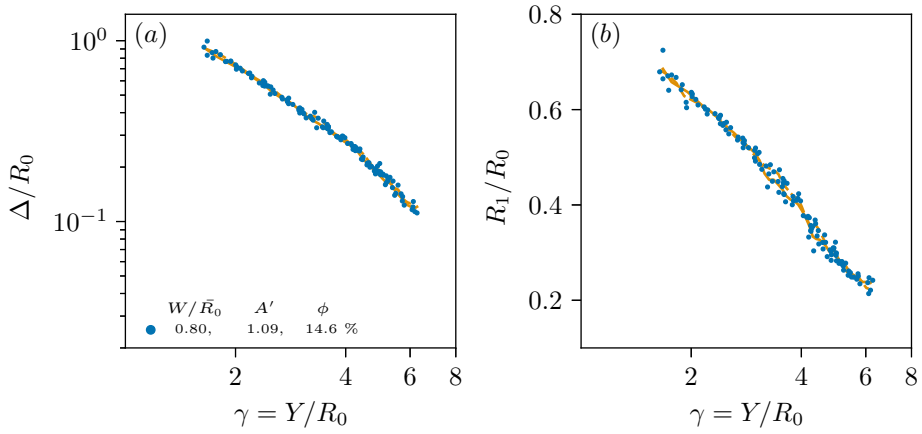

Figure 6: (a) Normalised displacement plotted against standoff distance. (b) Normalised rebound radius plotted against standoff distance. Data are plotted for a porous plate with circular holes. Data for bubbles positioned between-holes are traced by solid lines and data for bubbles positioned above holes are traced by dashed lines.

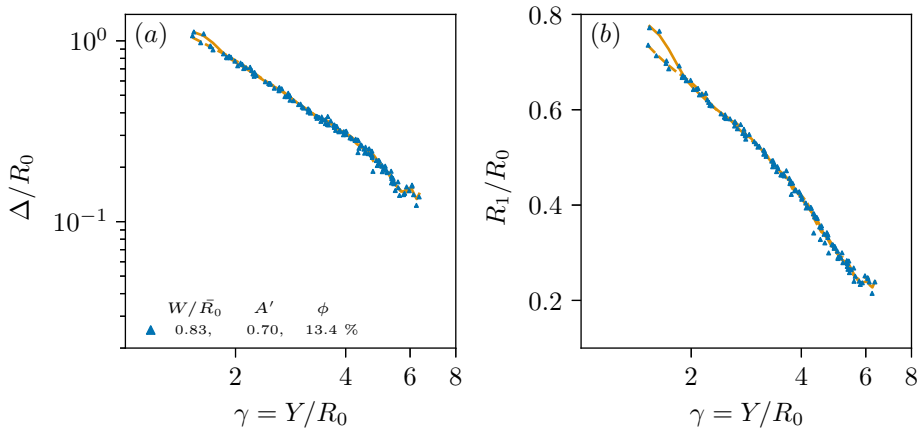

Figure 7: (a) Normalised displacement plotted against standoff distance. (b) Normalised rebound radius plotted against standoff distance. Data are plotted for a porous plate with triangular holes. Data for bubbles positioned between-holes are traced by solid lines and data for bubbles positioned above holes are traced by dashed lines.

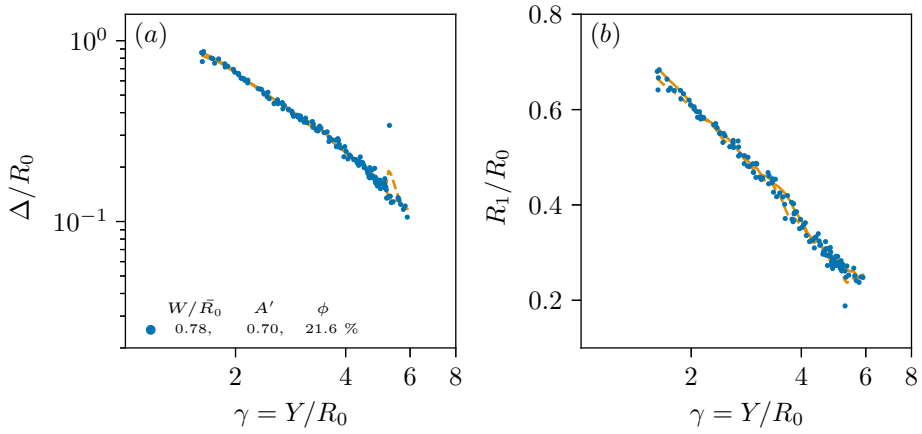

Figure 8: (a) Normalised displacement plotted against standoff distance. (b) Normalised rebound radius plotted against standoff distance. Data are plotted for a porous plate with circular holes. Data for bubbles positioned between-holes are traced by solid lines and data for bubbles positioned above holes are traced by dashed lines.

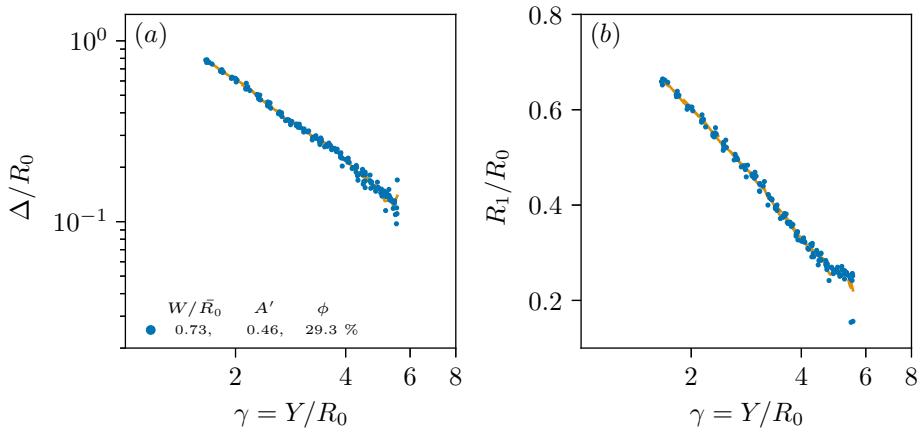

Figure 9: (a) Normalised displacement plotted against standoff distance. (b) Normalised rebound radius plotted against standoff distance. Data are plotted for a porous plate with circular holes. Data for bubbles positioned between-holes are traced by solid lines and data for bubbles positioned above holes are traced by dashed lines.

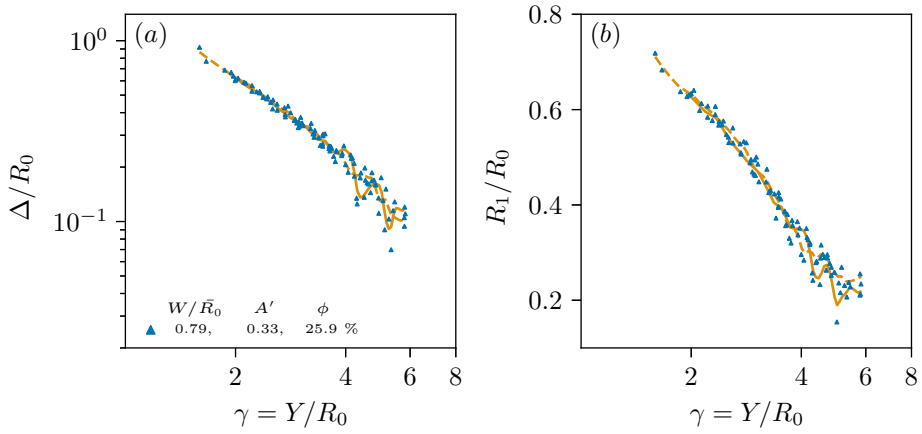

Figure 10: (a) Normalised displacement plotted against standoff distance. (b) Normalised rebound radius plotted against standoff distance. Data are plotted for a porous plate with triangular holes. Data for bubbles positioned between-holes are traced by solid lines and data for bubbles positioned above holes are traced by dashed lines.

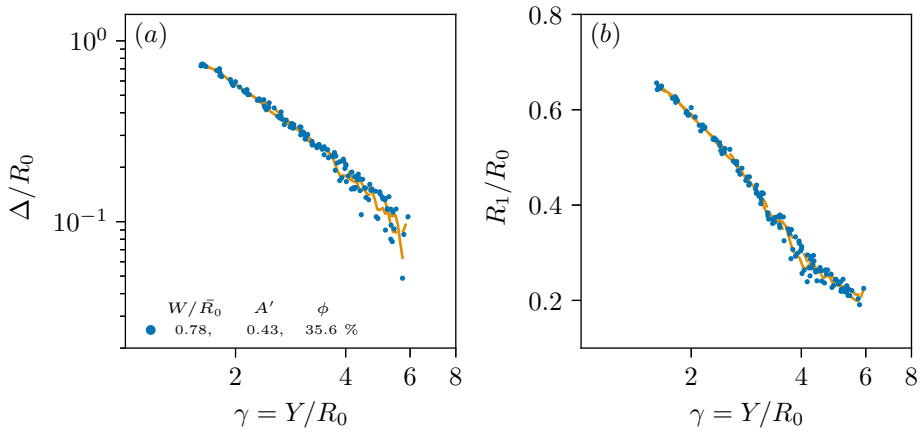

Figure 11: (a) Normalised displacement plotted against standoff distance. (b) Normalised rebound radius plotted against standoff distance. Data are plotted for a porous plate with circular holes. Data for bubbles positioned between-holes are traced by solid lines and data for bubbles positioned above holes are traced by dashed lines.

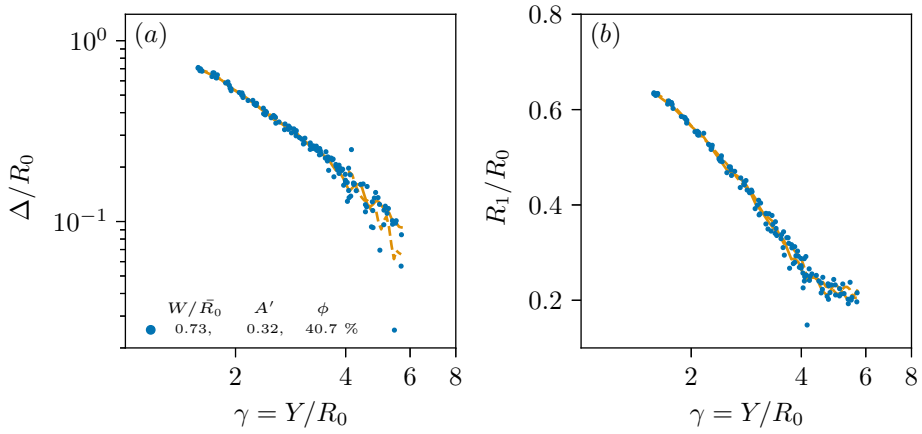

Figure 12: (a) Normalised displacement plotted against standoff distance. (b) Normalised rebound radius plotted against standoff distance. Data are plotted for a porous plate with circular holes. Data for bubbles positioned between-holes are traced by solid lines and data for bubbles positioned above holes are traced by dashed lines.

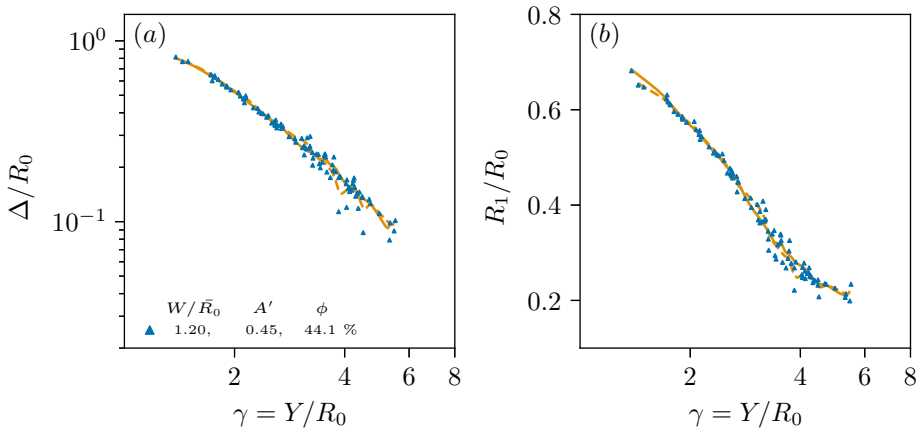

Figure 13: (a) Normalised displacement plotted against standoff distance. (b) Normalised rebound radius plotted against standoff distance. Data are plotted for a porous plate with triangular holes. Data for bubbles positioned between-holes are traced by solid lines and data for bubbles positioned above holes are traced by dashed lines.

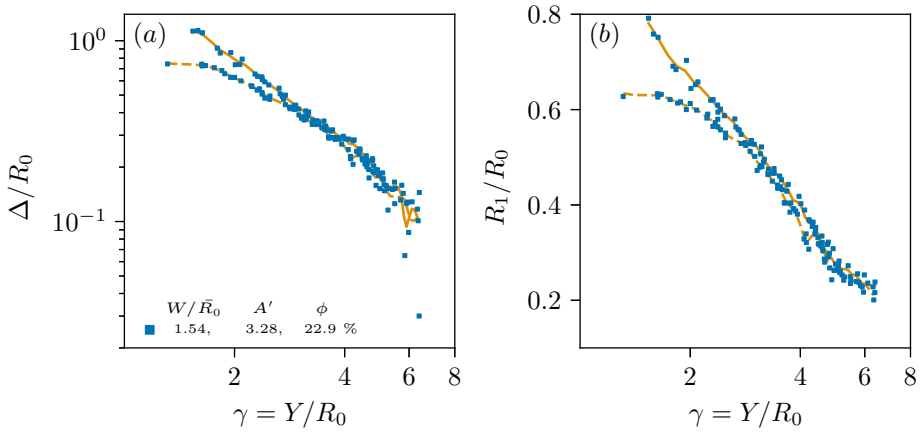

Figure 14: (a) Normalised displacement plotted against standoff distance. (b) Normalised rebound radius plotted against standoff distance. Data are plotted for a porous plate with square holes. Data for bubbles positioned between-holes are traced by solid lines and data for bubbles positioned above holes are traced by dashed lines.

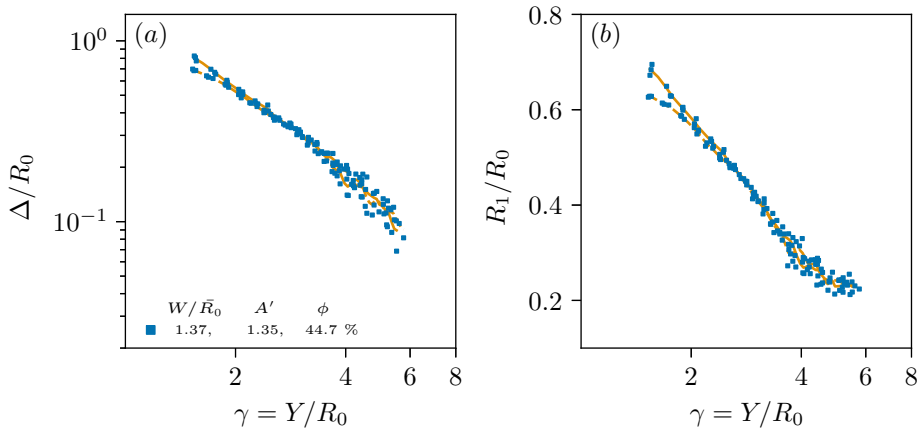

Figure 15: (a) Normalised displacement plotted against standoff distance. (b) Normalised rebound radius plotted against standoff distance. Data are plotted for a porous plate with square holes. Data for bubbles positioned between-holes are traced by solid lines and data for bubbles positioned above holes are traced by dashed lines.

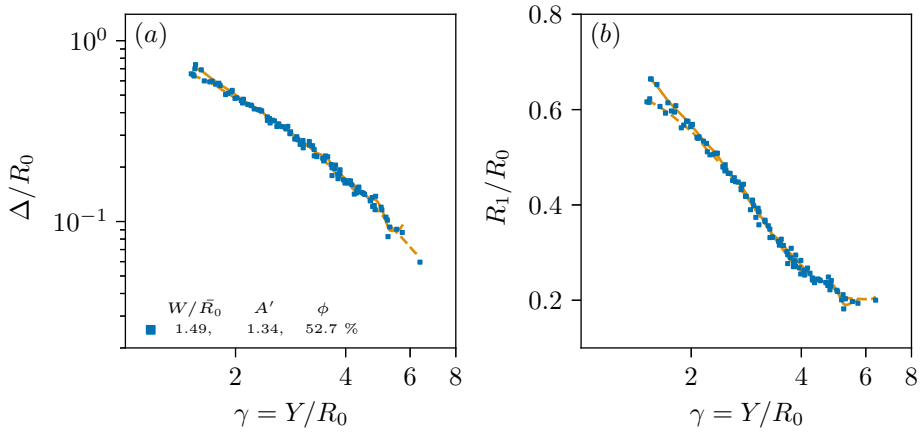

Figure 16: (a) Normalised displacement plotted against standoff distance. (b) Normalised rebound radius plotted against standoff distance. Data are plotted for a porous plate with square holes. Data for bubbles positioned between-holes are traced by solid lines and data for bubbles positioned above holes are traced by dashed lines.

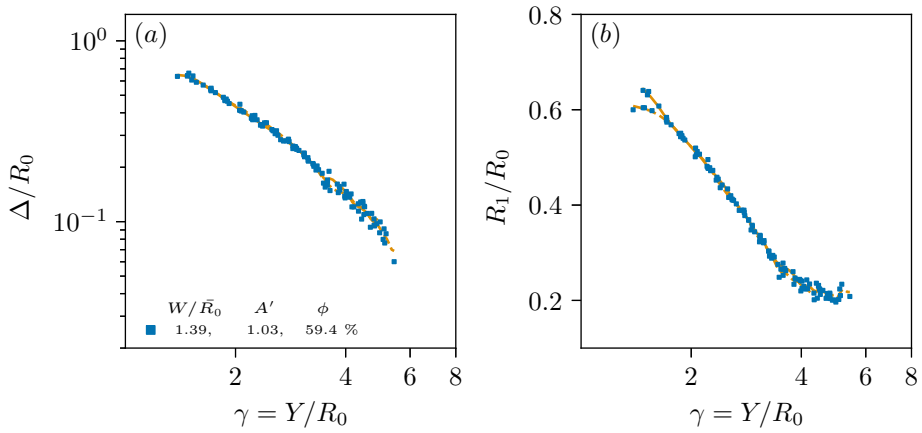

Figure 17: (a) Normalised displacement plotted against standoff distance. (b) Normalised rebound radius plotted against standoff distance. Data are plotted for a porous plate with square holes. Data for bubbles positioned between-holes are traced by solid lines and data for bubbles positioned above holes are traced by dashed lines.

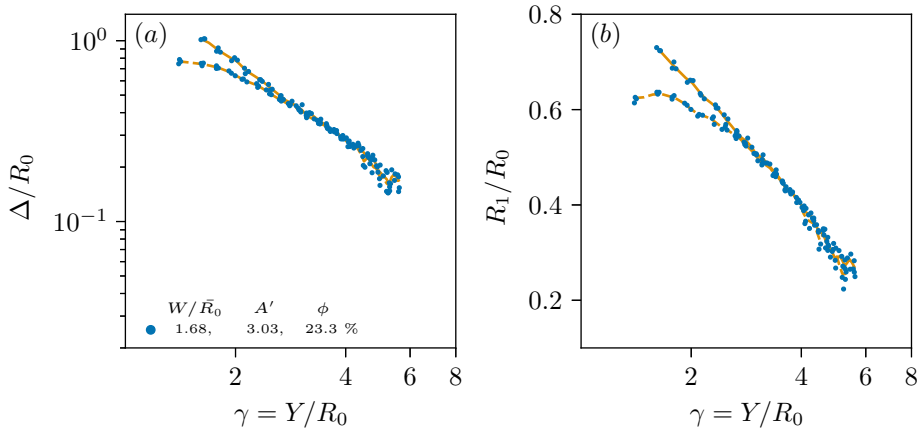

Figure 18: (a) Normalised displacement plotted against standoff distance. (b) Normalised rebound radius plotted against standoff distance. Data are plotted for a porous plate with circular holes. Data for bubbles positioned between-holes are traced by solid lines and data for bubbles positioned above holes are traced by dashed lines.

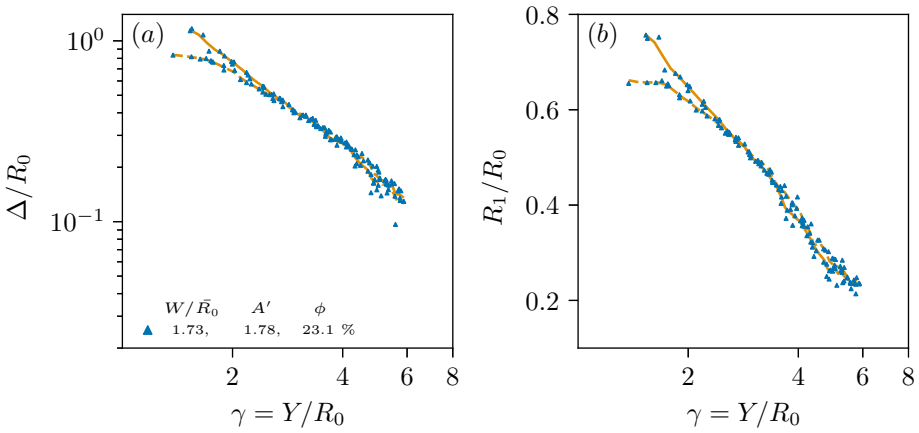

Figure 19: (a) Normalised displacement plotted against standoff distance. (b) Normalised rebound radius plotted against standoff distance. Data are plotted for a porous plate with triangular holes. Data for bubbles positioned between-holes are traced by solid lines and data for bubbles positioned above holes are traced by dashed lines.

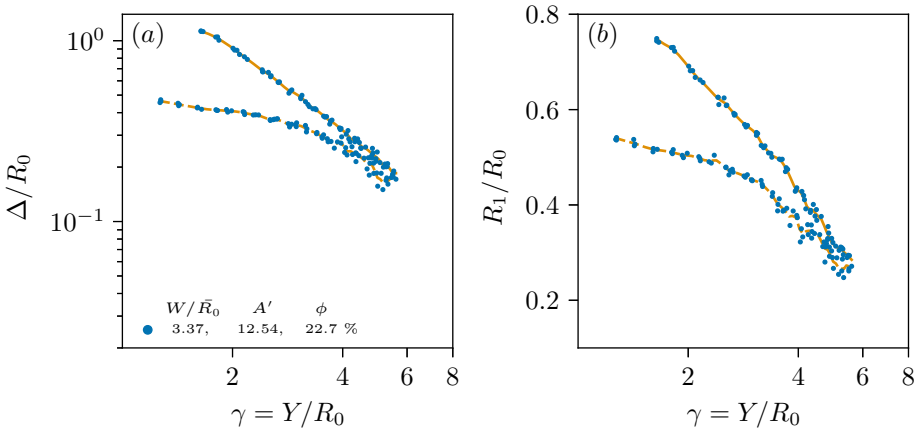

Figure 20: (a) Normalised displacement plotted against standoff distance. (b) Normalised rebound radius plotted against standoff distance. Data are plotted for a porous plate with circular holes. Data for bubbles positioned between-holes are traced by solid lines and data for bubbles positioned above holes are traced by dashed lines.

4 Anisotropy vs standoff from numerical model

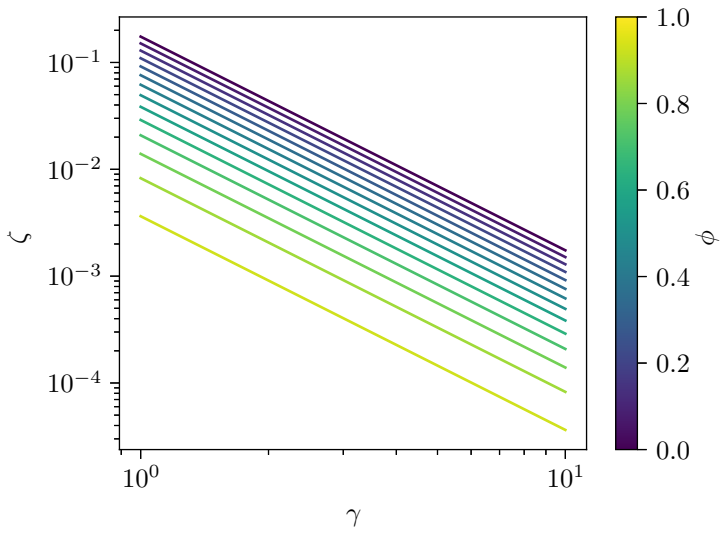

Figure 21: Anisotropy parameter ζ plotted against standoff distance γ for a range of void fractions ϕ using the boundary element method. The gradient of all lines are -2 to within four decimal places.

References

Andrews, Elijah D., Fernández Rivas, David & Peters, Ivo R. 2020 Cavity collapse near slot geometries. *Journal of Fluid Mechanics* **901**, A29.